Ballistic aggregation in systems of inelastic particles: Cluster growth, structure, and aging

Subhajit Paul and Subir K. Das*

Theoretical Sciences Unit, Jawaharlal Nehru Centre for Advanced Scientific Research, Jakkur P.O., Bangalore 560064, India

(Received 10 November 2016; revised manuscript received 16 March 2017; published 5 July 2017)

We study far-from-equilibrium dynamics in models of freely cooling granular gas and ballistically aggregating compact clusters. For both the cases, from event-driven molecular dynamics simulations, we have presented detailed results on structure and dynamics in space dimensions $d = 1$ and 2. Via appropriate analyses it has been confirmed that the ballistic aggregation mechanism applies in $d = 1$ granular gases as well. Aging phenomena for this mechanism, in both the dimensions, have been studied via the two-time density autocorrelation function. This quantity is demonstrated to exhibit scaling property similar to that in the standard phase transition kinetics. The corresponding functional forms have been quantified and the outcomes have been discussed in connection with the structural properties. Our results on aging establish a more complete equivalence between the granular gas and the ballistic aggregation models in $d = 1$.

DOI: 10.1103/PhysRevE.96.012105

I. INTRODUCTION

Structure and dynamics during cooling in systems of inelastically colliding particles have been of much research interest [1–23]. An importance of this topic stems from the relevance of it in the process of agglomeration of cosmic dust [21,22]. Two models in this context have been of significant importance, viz., the granular gas model (GGM) and the ballistic aggregation model (BAM). In the BAM, following a collision between two freely moving clusters, the colliding partners form a single larger object. In one dimension this corresponds to the sticky gas. While collisions trigger clustering immediately in the case of BAM, for the GGM (with coefficient of restitution $0 < e < 1$) the system remains in a homogeneous density state during an initial period, referred to as the homogeneous cooling state (HCS) [3,18]. The dynamics in the latter then crosses over to an inhomogeneous cooling state (ICS) [3], where particle-poor and particle-rich domains coexist. Time scale for such a crossover gets shorter with the decrease of e. These domains or clusters may grow for an indefinite period of time, if the system size is thermodynamically large [23]. Thus, even if not a phase transition, it is quite natural to study the clustering phenomena in these models from the perspectives of phase transition kinetics [24–26].

Like in phase transitions, in the case of a collection of inelastic particles also, considered to be hard spheres in many theoretical studies, power-law growths,

$$\ell \sim t^{\alpha}, \tag{1}$$

of the average domain length (ℓ), with time (t), have been observed [5,8–11,13]. In phase transitions, ℓ can be connected to the interfacial energy. Even though a connection with interfacial energy does not exist here, for the BAM the average cluster mass ($m \sim \ell^d$, d being the space dimension) has been related with the average kinetic energy (E) [21] as

$$m \sim \frac{1}{E} \sim t^{\frac{2d}{d+2}}. \tag{2}$$

Despite these and other advancements, many questions in this area remain open, including issues related to the equivalence between the BAM and the GGM.

In $d = 1$, validity of Eq. (2) has been confirmed, via simulations, for the BAM as well as the GGM [6,7,10,11,21]. In higher dimensions, on the other hand, the status is not satisfactory with respect to the equivalence between the two models. Even though the time-dependence of E has been reported to be consistent with Eq. (2), for the growth of m in the GGM there exists evidence for dimension independence [13]. This raises concern whether the complete validity of Eq. (2) in $d = 1$, for both the models, is accidental. Thus, even in this dimension, direct confirmation of the mechanism of growth, if possible, in the GGM is essential, to draw a conclusion on this matter [6]. For $d > 1$, strictly speaking, even for the BAM the time dependence in Eq. (2) requires modification, since in that case one expects isolated fractal clusters [27] with fractal dimension d_f ($<d$) such that $m \sim \ell^{d_f}$. This fact is not included in Eq. (2), and due to technical difficulties, in existing simulation studies also spherical (compact) structural assumption [14,15] of the growing clusters became necessary.

Furthermore, as discussed above, while some aspects of growth have been studied, aging property [26,28–34] of the density-field evolution did not receive attention for these models, though important [35]. We stress that knowledge of aging, along with its connection to pattern and growth, is crucial to the understanding of out-of-equilibrium systems. To the best of our knowledge, there exists only one study [36] that addresses scaling property of a two-time correlation function, to be introduced in the next section, in the context of aging in granular-matter. This, however, considers aging in a different quantity, for a model different from the ones considered here.

Various scaling aspects that have been established with respect to aging are related to the approach of a far-from-equilibrium system to an equilibrium state, like in phase transitions. Given that the systems of inelastically colliding particles are always out of equilibrium, examination of the validity of these properties in such systems should be of genuine importance. If scaling exists, it is of interest then to compare the scaling functions associated with the GGM and the BAM cases, to establish a more complete equivalence between the two models.

*das@jncasr.ac.in

In this work, our primary objective is to identify the scaling property of the above-mentioned two-time correlation function in situations where growth occurs via ballistic aggregation. For this purpose, it has been shown, via a state-of-the-art dynamic renormalization group theoretical method of analysis [37], that the growth law for the one-dimensional GGM in ICS is same as that for the BAM. In this dimension, we also directly show that the mechanism of aggregation in the GGM is indeed ballistic. These, along with our results on aging, establish a more complete equivalence between the GGM and the BAM in $d = 1$. On the other hand, in $d = 2$ we have pointed out vast differences between the structure and growth in the GGM and the corresponding theoretical expectations for the BAM. In the latter dimension, thus, for aging property, we work only with the BAM. In $d = 2$, via accurate analyses, we also check the validity of a hyperscaling relation, which combines the exponents for the decay of kinetic energy and the growth of clusters, for the BAM.

The balance of the paper is organized in the following way. In Sec. II we provide an overview of various scaling properties related to nonequilibrium dynamics during phase transitions. We discuss the models and methods in Sec. III. The results are presented in Sec. IV. Finally, Sec. V concludes the paper with a summary and outlook.

II. BACKGROUND OF SCALING PROPERTIES

In problems of phase transitions [24], having been quenched from a homogeneous state to a state inside the miscibility gap, as a system proceeds toward the new equilibrium, one is interested in understanding the domain pattern [24], its growth rate [24], and aging [26]. As stated above, typically the growth occurs in a power-law fashion, with the growth exponent α having dependence upon transport mechanism, system dimension, number of components of the order parameter, and the conservation of the total value of the latter over time. For the present problem, like in a vapor-liquid transition, the relevant order parameter is related to the local density field, total value of which is a conserved scalar quantity.

Typically there exists self-similarity in the growth process [24], i.e., the patterns at two different times are similar to each other, in a statistical sense, apart from a change in the length scale. An appropriate method of characterization of pattern is to calculate the two-point equal-time correlation function [24],

$$C(\vec{r},t) = \langle \psi(\vec{r},t)\psi(\vec{0},t)\rangle - \langle \psi(\vec{r},t)\rangle\langle \psi(\vec{0},t)\rangle, \qquad (3)$$

where ψ is a space- ($\vec{r}$) and time-dependent order parameter. In the next section we will provide description on how, in the present problem, ψ can be obtained from the density field. The angular brackets in Eq. (3) correspond to statistical averaging. For an isotropic pattern, e.g., when there is no external bias, the value of the correlation function depends only on the scalar distance between two points. In that case, in addition to the averaging over different initial configurations, one can take the route of spherical averaging as well. The directly accessible quantity in experiments [24], however, is the structure factor $S(k,t)$, Fourier transform of $C(r,t)$, k being the magnitude of the wave vector.

The above-mentioned self-similarity is reflected in the scaling properties of $C(r,t)$ and $S(k,t)$ as [24]

$$C(r,t) \equiv \tilde{C}(r/\ell), S(k,t) \equiv \ell^d \tilde{S}(k\ell), \qquad (4)$$

where $\tilde{C}$ and $\tilde{S}$ are time-independent master functions [24]. In the area of kinetics of phase transitions, there has been strong interest in obtaining analytical expressions for these quantities [24,26]. While significant success has been achieved for the situation where the order parameter is a nonconserved quantity, for the case of the conserved order parameter only partial understanding has been obtained. For example, behavior of $S(k,t)$ is analytically known only in the small and large k limits.

For the study of aging property, one considers a two-time autocorrelation function [28,29],

$$C_{\rm ag}(t,t_w) = \langle \psi(\vec{r},t)\psi(\vec{r},t_w)\rangle - \langle \psi(\vec{r},t)\rangle\langle \psi(\vec{r},t_w)\rangle, \qquad (5)$$

where t_w ($\leqslant t$) and t are referred to as the waiting time (or the age of the system) and the observation time, respectively [26]. Unlike the equilibrium situation, there is no time translation invariance in an evolving system. The decay of $C_{\rm ag}(t,t_w)$ gets slower with the increase of t_w, which can be seen by plotting it versus $t - t_w$. This reflects the fact that relaxation in an aged system is weaker than that in an younger system. In kinetics of phase transitions, $C_{\rm ag}(t,t_w)$ follows a scaling relation [26,28],

$$C_{\rm ag}(t,t_w) \equiv \tilde{C}_{\rm ag}(x); \quad x = \ell/\ell_w, \qquad (6)$$

where ℓ_w is the domain size at t_w and $\tilde{C}_{\rm ag}$ is a master function [26]. In absence of hydrodynamics, it has been shown, via analytical theories and computer simulations [26,28,29,34,38–40], that the decay of $\tilde{C}_{\rm ag}$ follows power-law:

$$\tilde{C}_{\rm ag} \sim x^{-\lambda}. \qquad (7)$$

Fisher and Huse (FH) [28] provided bounds on the values of the exponent λ as

$$\frac{d}{2} \leqslant \lambda \leqslant d. \qquad (8)$$

The power-law scaling and the bounds can be justified from the consideration of the values of the average order parameter within any fixed region at times t and t_w. However, while the lower bound works, the upper bound is less strict and there have been reports of violation of it [30,34,39]. Later, Young, Rao, and Desai (YRD) [30] provided a stricter lower bound, by taking the structural properties into consideration. This bound reads

$$\lambda \geqslant \frac{d+\beta}{2}, \qquad (9)$$

where β is the exponent for the small wave-number power-law behavior of the structure factor:

$$S(k,t) \sim k^{\beta}. \qquad (10)$$

Using the structure factors at times t and t_w, and exploiting the scaling property of $S(k,t)$ [see Eq. (4)], YRD obtained

$$C_{\rm ag}(t,t_w) \leqslant \ell^{d/2} \int_0^{2\pi/\ell} dk k^{d-1} [S(k,t_w)\tilde{S}(k\ell)]^{1/2}. \qquad (11)$$

The bound follows when Eq. (10), for the small k behavior of $S(k,t_w)$, is used in the above expression. In the case of

nonconserved order parameter $\beta = 0$ and the YRD bound coincides with the FH lower bound [30]. For phase separation in systems with conserved order parameter [30] $\beta > 0$, and so the YRD bound is expected to be more strict. In Ising-like systems, where coarsening occurs via diffusive transport of material, it has been shown that the power-law scaling and the YRD bound are obeyed [30,39].

Investigation of these facts in systems consisting of inelastic particles should be of genuine interest, to obtain a broader picture with respect to the concepts of nonequilibrium statistical mechanics, since these systems continuously dissipate kinetic energy. We show that, irrespective of the dimension, the above power-law scaling property of the autocorrelation function holds for both the models, at least when the growth occurs via ballistic aggregation. The corresponding exponents have been estimated and are seen to follow the YRD bound.

III. MODELS AND METHODS

For the GGM, we use the following update rule for the (equisized, hard-core) particle velocities. The post- and precollisional velocities of the particles are related via [3,41,42]

$$\vec{v}_i' = \vec{v}_i - \left(\frac{1+e}{2}\right)[\hat{n}\cdot(\vec{v}_i - \vec{v}_j)]\hat{n}, \tag{12}$$

$$\vec{v}_j' = \vec{v}_j - \left(\frac{1+e}{2}\right)[\hat{n}\cdot(\vec{v}_j - \vec{v}_i)]\hat{n}, \tag{13}$$

where ($'$) stands for the post event, $\vec{v}_i$ and $\vec{v}_j$ are velocities of particles i and j, respectively, and $\hat{n}$ is the unit vector in the direction of the relative position of the particles i and j. With this model, we perform event-driven [41,42] molecular dynamics simulations, where an event is a collision. In this method, between two collisions, since there are no interparticle interaction or external potential, particles move with constant velocities. For every event the collision partners and the time are appropriately identified [41].

For the BAM case [21], following every collision, mass of the product particle increases, which was appropriately incorporated in the collision rule. For the BAM in $d = 2$ we use the same circular approximation for the structure of the product clusters as in the previous studies [43], which will be briefly discussed later. Typically, in such event-driven simulations time is specified in two different ways, viz., by using the number of collisions per particle (τ) and by calculating the actual time (t), the latter can be obtained by keeping track of the free time between the collisions. In this work, we will use the latter.

A serious problem faced in event-driven simulations of the GGM is the inelastic collapse [44]. This phenomenon is related to the fact that, for very low values of the relative velocity, collisions keep occurring only among particles within a small group of neighbors. This essentially stops the progress of time. The problem is more severe in lower dimension, since fewer particles are needed to satisfy the corresponding condition. Such singularity in collision numbers can be avoided in two ways, viz., by setting the value of e, for the collision partners with relative speed less than a threshold value δ, to either 0 or 1. We adopt the latter [6,44–46], given that in the experimental situation value of e increases with the decrease of the relative velocity [10–12,47]. In $d = 2$, however, we set δ to zero, since the problem is less severe in higher dimension, and so significantly large cluster sizes can be accessed without encountering such collapse.

All our results will be presented from simulations with periodic boundary conditions, by fixing the starting value of density of particles to $\rho = N/L^d = 0.30$, N being the number of particles and L the linear dimension of the system, except for the $d = 2$ GGM, for which we choose $\rho = 0.37$. Given that the particles have diameter unity (to start with), in $d = 2$ these numbers for particle density correspond to packing fractions 0.235 (BAM) and 0.29 (GGM).

In the case of GGM, clusters were appropriately identified as regions with density above a critical value ρ_c (=0.5). Higher values of ρ_c also provide similar results, deviating from each other only by constant multiplicative factors. The end-to-end distance for a cluster, along any direction, provides a cluster length (ℓ_c). In $d = 1$, the number of particles within these boundaries is the mass (m_c) of that cluster. In $d = 2$, one needs to appropriately identify the closed boundaries of the clusters, to calculate the mass. For the BAM case, information on the cluster length and mass are contained in the particle radius. The average values of the above-mentioned quantities were obtained from the first moments of the distributions of ℓ_c and m_c. Ideally, ℓ should equal $m^{1/d}$, but in the case of GGM it takes time for a cluster to settle down to a particular density value. Thus, equality holds only at late time. For the calculation of the correlation functions and structure factors [8,9], the order-parameter ψ at a lattice point (for this purpose the continuum systems were mapped onto a square lattice) was assigned a value $+1$ if the density (for the GGM this was calculated by counting the number of particles within a preassigned radius, the point of interest being the center of the corresponding circle) there was higher than ρ_c, else -1. The average length can be calculated from the scaling property of $C(r,t)$ or $S(k,t)$ as well.

IV. RESULTS

We divide the section into subparts A and B. In subsection A, we present results from $d = 1$. The $d = 2$ results are shown in subsection B.

A. $d = 1$

As mentioned above, in this dimension, via accurate analyses, we first confirm the equivalence between the BAM and the GGM, with respect to the energy decay, the growth law, and the corresponding mechanism. These results are followed by those for aging property. As we will see, the latter, in addition to being of separate importance, will make the above-mentioned equivalence more complete.

In Fig. 1(a) we show the time dependence of energy, for both the models, on a log-log scale. The BAM results, for energy and mass [see Fig. 1(b)], are already understood. Nevertheless, we present these here, for the sake of completeness, as well as to facilitate the discussion that follows. For the GGM, results for a few different cutoff values of the relative velocity are shown. For this model, in this dimension, all our results correspond to $e = 0.5$. After a minor disagreement over a brief

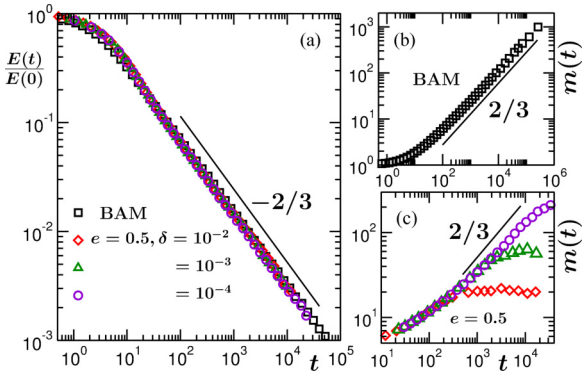

FIG. 1. (a) Decay of energy in the BAM and the GGM are plotted vs. time. For the GGM, value of e has been fixed to 0.5 and results for several choices of δ are presented. (b) Average cluster mass, m, is plotted vs. time, for the BAM. (c) Same as (b) but for the GGM with multiple values of δ as in (a). The solid lines in these figures correspond to various power laws, exponents for which are mentioned. The starting number of particles for the BAM and the GGM are, respectively, 160 000 and 10 000. Rest of the simulations for the GGM are done with 20 000 particles and $\delta = 5 \times 10^{-5}$. All results correspond to $d = 1$.

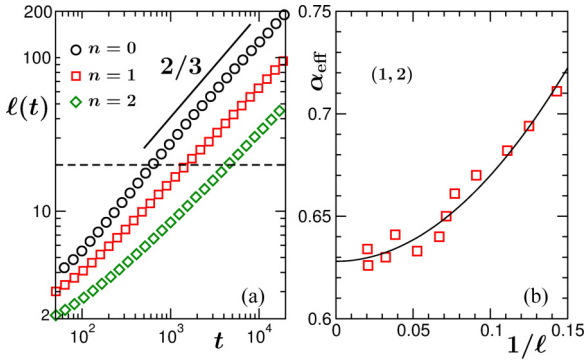

FIG. 2. (a) Plots of ℓ vs. t for three different stages of renormalization. The dashed horizontal line is for the extraction of times for the same length at different levels of renormalization. The solid line represents a power-law with exponent 2/3. (b) Plot of the effective exponent, obtained via the renormalization-group analysis using the combination $n = 1$ and 2, vs. the inverse of the original length. The solid line is a quadratic fit to the simulation data. All results correspond to the GGM in $d = 1$.

initial period (corresponding to HCS in the GGM), results from the two models fall on top of each other and exhibit power-law behavior over several decades in time, with the expected exponent $-2/3$.

In Fig. 1(b) we plot m as a function of t, on a log-log scale, for the BAM case. This shows a power-law growth with exponent 2/3, validating Eq. (2). The m versus t results for the GGM are shown in Fig. 1(c), for the same values of δ as in Fig. 1(a). An interesting observation here is that, for the GGM, even though the energy decay follows $t^{-2/3}$ behavior till late for all values of δ, the picture is different for the growth of mass. The growth stops earlier for larger value of δ, while energy decay continues with the predicted functional form. This should not be a finite-size effect, since the saturation is δ dependent. Rather, this has connection with the late time declusterization phenomena [10,11] that has been observed for relative-velocity dependent e. Furthermore, the m versus t data, particularly for larger values of δ, do not appear completely consistent with the exponent 2/3, before saturation. This discrepancy can possibly be due to the presence of a substantial length at the beginning of the scaling regime. In such a situation, confirmation of an exponent, from a log-log plot, requires data over several decades in time [48]. In absence of that, alternative accurate method of analysis is needed to obtain correct value of the exponent [37,48,49]. In any case, the observations above, with respect to the saturation of m, further justify the need for direct identification of the growth mechanism. Before moving to that, we will accurately quantify the growth law. For this purpose, in the following we will work with the length, rather than the mass, since for the aging study we intend to use the ratio of lengths as the scaling variable. Unless otherwise mentioned, in this subsection, all our results for the GGM, from here on, will be presented for $\delta = 5 \times 10^{-5}$.

We use a renormalization-group method of analysis [37] for the accurate quantification of the growth in the GGM. We consider a Kadanoff-type block transformation [50] of the order parameter. For this purpose, as mentioned in the context of calculation of the correlation functions, we have mapped the density field to $\psi = \pm 1$, on a lattice. The blocking exercise then becomes similar to that for the Ising model [24]. At successive iterations of the transformation, order parameter over a length of b particle diameters is averaged over and represented by a single point. This reduces the system size by a factor b, for which we choose the value 2. Thus, a particular value of ℓ in different levels (n) of renormalization will be obtained at different times, viz., for $n = p$ and $p + 1$ one writes [37]

$$\ell(p,t) = \ell(p+1, b^{1/\alpha} t). \tag{14}$$

This is demonstrated in Fig. 2(a), where, in addition to the original data ($n = 0$), we have shown length versus time plots for renormalizations with $n = 1$ and 2. The horizontal line in this figure is related to the estimation of times for the same length scale at different values of n. From the shifting or scaling of time, due to the scaling in length, the growth exponent can be estimated. However, because of technical reasons, the true exponent will be realized only in the limit $\ell \to \infty$ and at finite time we will denote it by $\alpha_{\rm eff}$.

Estimated values of $\alpha_{\rm eff}$, from the combination involving $n = 1$ and 2, are presented in Fig. 2(b), versus $1/\ell$, which indeed have time dependence [51]. Such time dependence is due to the nonscaling early time transient and presence of a large off-set when scaling is reached. In situations like this, as already stated, α should be estimated from the convergence of the data in the $\ell \to \infty$ limit. By looking at the trend of the data set, we have fitted it to the form $\alpha_{\rm eff} = \alpha + a/\ell^2$, which provides convergence to $\alpha \simeq 0.63$. This is very close to the ballistic aggregation [21] value 2/3. To check whether the minor deviation of the simulation data from the theoretical expectation is a true fact, one needs to study other values of e as well. Such a systematic study we leave out for a future work. The deviation could be due to the finite-size effects and δ-dependent saturation.

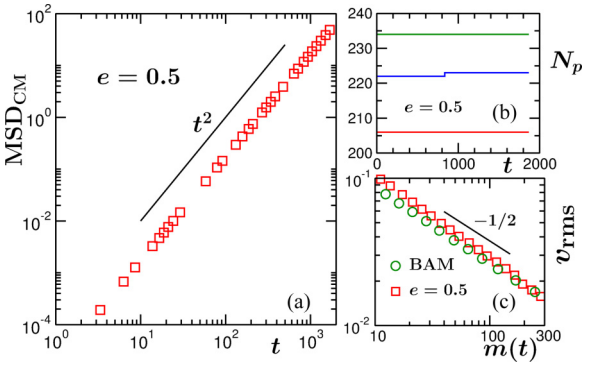

FIG. 3. (a) Mean-squared-displacement of the center of mass of a typical cluster, for the GGM, is plotted vs. time, on a log-log scale. The solid line corresponds to ballistic motion. (b) Number of particles in a few different clusters, for the GGM, are plotted vs. translated time, before they undergo collisions. (c) Root-mean-squared velocity of the clusters are plotted vs. m, for both the models. The solid line is a power-law decay, exponent being mentioned. All results are from $d = 1$.

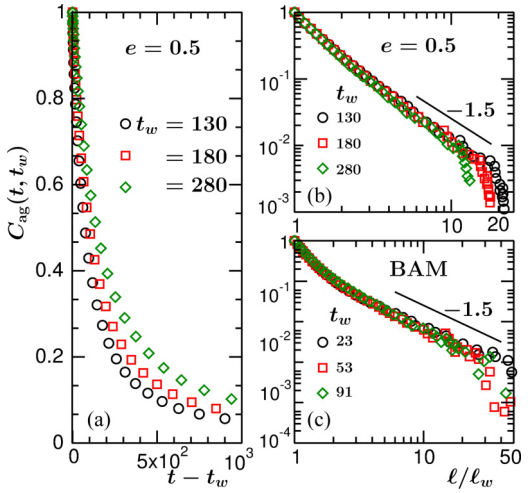

FIG. 4. (a) Plots of the autocorrelation function, vs. $(t - t_w)$, for three different choices of t_w, as mentioned, for the $d = 1$ GGM. (b) Log-log plots of $C_{ag}(t,t_w)$ vs. ℓ/ℓ_w, using the data sets in (a). (c) Same as (b) but for the $d = 1$ BAM case. The values of t_w are mentioned on the figure. The solid lines in (b) and (c) represent power-law decays with exponent $\lambda = 1.5$.

Having identified the growth exponent for the GGM, we, in Fig. 3, identify the mechanism. The growth exponent 2/3 can be obtained from a (nonequilibrium) kinetic theory for ballistic aggregation [21,27,52]. As the name suggests, growth in this mechanism occurs due to collisions among clusters and between collisions the clusters move with constant velocities. Since the particles in our models are noninteracting (beyond the hard-core diameter), it is understandable that the clusters in the BAM will move ballistically between collisions. In the GGM case also, following more and more collisions, particles within a cluster may move parallel to each other, providing collective directed motion. However, growth in this case may as well occur due to random deposition of particles on the clusters when the latter objects move through a reasonably high-density vapor region. It is then necessary to check, if at a late enough time the motion of the clusters, during the interval between two big mass enhancing collisions, are ballistic and during that period the growth of the clusters is negligible.

In Fig. 3(a) we show the mean-squared displacement of the center of mass (CM), MSD$_{CM}$, of a cluster, calculated as [53]

$$\mathrm{MSD}_{CM} = \langle |\vec{R}_{CM}(t) - \vec{R}_{CM}(0)|^2 \rangle, \tag{15}$$

$\vec{R}_{CM}$ being the time-dependent location of the CM of the cluster, for the GGM, over an extended period of time, before it undergoes a collision with another cluster. On the log-log scale, a very robust t^2 behavior is visible, implying ballistic motion [53]. In Fig. 3(b) we show the numbers of particles in a few clusters, as a function of time, translated by subtracting the times at the beginning of the observations. The "constant" values over long periods confirm that the mechanism of growth in the GGM is indeed ballistic aggregation.

The mass part of Eq. (2) can be derived from [21,27,52]

$$\frac{dn_c}{dt} = -\ell^{d-1} v_{rms} n_c^2, \tag{16}$$

where n_c is the cluster density and v_{rms} is the root-mean-squared velocity of the clusters. An exponent 2/3 requires $v_{rms} \sim m^{-1/2}$, an outcome for uncorrelated cluster motion [52].

In Fig. 3(c) we plot v_{rms} versus m, for the BAM as well as the GGM. Results from both the models show consistency with the requirement. The reasonable agreement of v_{rms} with the $m^{-1/2}$ form, that is observed, should, however, be checked for other values of density and e (latter applies to the GGM). Any deviation, though does not invalidate the ballistic aggregation, can change the growth exponent. Here, as a passing remark, we mention that for the ballistic aggregation of fractal clusters in d dimensions, with $v_{rms} \sim m^{-\gamma}$, the exponent for the time dependence of mass will have the form

$$\zeta = \frac{d_f}{1 - d + d_f(1 + \gamma)}, \tag{17}$$

if Eq. (16) is a good starting point. Given that for the present problem $d_f = d = 1$ and our estimate of γ for the GGM is 0.55, we obtain $\zeta = 0.645$, which is in agreement with the conclusion from Fig. 2(b). We find similar value for ζ from the analysis of the instantaneous exponent. For $d = 2$, we will adopt this method, instead of the renormalization group.

Next, we present results for the aging property [26,28]. We stress again, not only in the granular matter context, to the best of our knowledge, aging has not been studied previously for ballistic aggregation in any other system. In Fig. 4(a) we show $C_{ag}(t,t_w)$ versus $t - t_w$, for a few different values of t_w, for the GGM. As expected, no time translation invariance is noticed, which is an equilibrium [53] (or steady-state) property. Sticky gas (BAM) results are similar (not shown). In Fig. 4(b) we show $C_{ag}(t,t_w)$ versus ℓ/ℓ_w, on a log-log scale, for the GGM. Nice collapse of data, for all chosen values of t_w, are seen, as in kinetics of phase transition. Deviations of the data sets from the master curve, appearing earlier for larger values of t_w, are due to finite-size effects [38]. In phase transitions, the system moves toward an equilibrium state. Interestingly, similar scaling is observed in the present case, despite the fact that the system is continuously dissipating

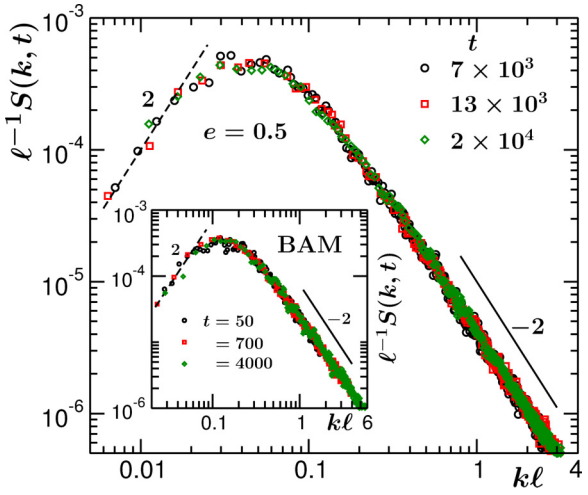

FIG. 5. Scaling plot of the equal-time structure factors for the $d = 1$ GGM. Here we have shown collapse of $S(k,t)/\ell(t)$, when plotted as a function of $y = k\ell(t)$, using data from three different times. Inset shows the same exercise as in the main frame but for the $d = 1$ BAM. In the main frame as well as in the inset, the dashed and the solid lines correspond to $\sim y^2$ and $\sim y^{-2}$, respectively.

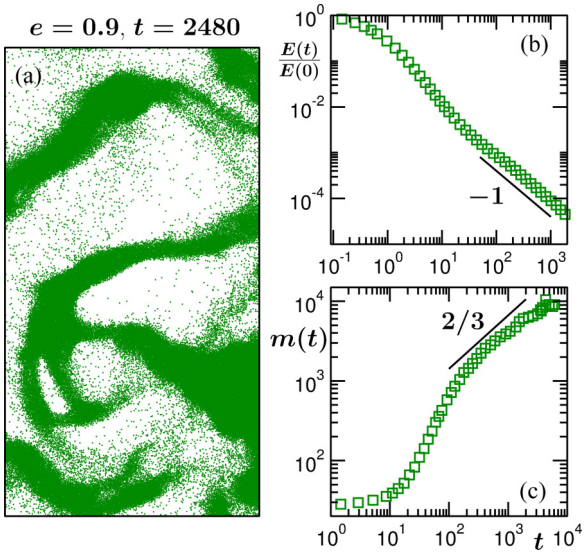

FIG. 6. (a) A snapshot during the evolution in GGM with $e = 0.9$ in $d = 2$. Only a part of the snapshot is shown. The particles are marked by dots. (b) Log-log plot of the energy as a function of t, for the system in (a). (c) Log-log plot of mass vs. time, for the GGM in (a). All results are obtained with $L = 512$. The solid lines in (b) and (c) represent power laws, exponents for which are mentioned.

kinetic energy. Corresponding plots for the BAM are shown in Fig. 4(c). Again, very good quality collapse is observed. In both the cases, power-law decays [28] [recall Eq. (7)] of the scaling function are observed for $x \gg 1$, the exponent values, mentioned on the figures, being same (or close to each other) in the two cases. This further confirms the equivalence between the BAM and the GGM. To check whether λ obeys the bound in Eq. (9), we analyze the structure.

In Fig. 5 we show the scaling plot of the structure factors, viz., we plot $\ell^{-1}S(k,t)$ versus $k\ell$, for the GGM. Nice collapse of data from all different times imply structural self-similarity [24]. The consistency of the long wave-vector data with k^{-2} imply validity of the Porod law [24,54,55],

$$S(k,t) \sim k^{-(d+1)}, \tag{18}$$

a consequence of short-distance singularity in $C(r,t)$, due to scattering from sharp interfaces. The small k behavior appears consistent with $\beta = 2$. The corresponding results for the BAM structure factor, shown in the inset of Fig. 5, are very similar. The value $\beta = 2$ was predicted [56] for coarsening in Ising-like systems in $d = 1$. The number is different for higher dimensions [57]. The dimension dependent values of β can be obtained [58] from dynamical equation of the structure factor (starting from the Cahn-Hilliard equation [58]) in k space, by arguing that for $d = 1$ thermal energy is dominant, whereas for $d > 1$ interfacial free energy takes over. Agreement of our results with such prediction is very interesting. The information on the consistency, for both short- and long-scale structures, between the GGM and the BAM, that these data sets convey, is further supportive of the presence of sharp interfaces, compact clusters, and ballistic aggregation in the GGM.

The observed value of β sets the lower bound for λ at 1.5. Thus, this bound is obeyed in both the cases and the actual values of the aging exponent, in fact, are very close to this lower bound. Here, note that violation of such power-law decay of the autocorrelation function was demonstrated recently [33,34], for advective transport in fluid phase separations. Even for conserved order parameter with diffusive dynamics, though power-law, the decays in $d > 1$ are observed [39] to be significantly faster than the ones provided by this (lower) bound (9). However, in the latter example, agreement with the bound gets better as the dimension decreases [39]. With the lowering of d, particularly for Ising kinetics, motion of the boundaries of domains (during no growth periods) gets restricted. However, since the mechanism is ballistic in the present problem, boundary movement does exist even during no growth period, though decreases with the increase of mass, thus time. Nevertheless, the agreement with the lower bound is rather close.

B. $d = 2$

In this subsection, first we briefly discuss the case of GGM, to convince ourselves that the growth in this case does not occur via the ballistic aggregation mechanism. Unlike the simulations of GGM in $d = 1$, we do not use any nonzero cutoff value (δ) for the relative velocity here. This is because, for high enough value of e, in this dimension, we are able to access relevant scaling regime without encountering an inelastic collapse [13].

In Fig. 6(a) we show an evolution snapshot for the $d = 2$ GGM with $e = 0.9$. Interesting pattern, consisting of coexisting particle-rich and particle-poor domains, is visible. A log-log plot of the kinetic energy in the system, as a function of t, is presented in Fig. 6(b). The initial decay (corresponding to HCS) is consistent with the prediction of Haff [18], $E \sim e^{-a\tau}$ (a is a constant; analytical curve is not shown). The late time data follow a power-law in t, with exponent -1. This is, thus, consistent with the prediction of Eq. (2). In Fig. 6(c), we show

a log-log plot of m versus t. The data in the late time scaling regime are seen to obey a power law, the exponent being $\lesssim 2/3$. Here we mention that in a previous work [13], via a finite-size scaling analysis, we had shown that the average domain length grows as t^{α}, with $\alpha \simeq 1/3$. The conclusion from Fig. 6(c) is, thus, in agreement with this earlier study. Nevertheless, given that for the GGM there exists possibility of continuous change of density within the domains, it is instructive to separately analyze the results for average mass [13].

Since Eq. (2) predicts inverse relationship between mass and energy, the kinetics of GGM is different from ballistic aggregation, particularly when the exponents do not follow even a hyperscaling relation [14,15] (see discussion below in the context of BAM). Matching of the exponent for energy decay [with Eq. (2)] is accidental. In the rest of the subsection, therefore, we focus only on the BAM. This is by keeping in mind that the primary objective is to study aging during ballistic aggregation.

There are different variants of models dealing with ballistic aggregation. For example, there exists interest in a model where ballistically moving particles from a source get deposited on a fixed substrate or seed. Such models are of relevance in situations like construction of vapor-deposited thin films. Corresponding structures are fractal [59]. In the present case, however, all the clusters move ballistically, between collisions. Simulation of such a BAM in $d > 1$ is not straightforward. This is because, if no deformation of the clusters is considered, highly fractal structures are expected in this situation as well. In that case, one needs to *a priori* identify the exact points of contact, for evolving the systems via collisions. This is a difficult task, particularly if the rotations of the clusters are considered. In the left frame of Fig. 7(a), we show a snapshot, obtained during an evolution of the BAM, without incorporating any deformation and considering only the translational motion of the clusters. A nice fractal pattern is seen. We have estimated the fractal dimension, which we discuss later.

Because of the above-mentioned difficulty in dealing with the actual physical scenario, researchers [14,15,43] have adopted a spherical structural approximation. In this method, after a collision between two spherical objects of diameters σ_1 and σ_2, the mass of the resulting cluster is (usually) uniformly distributed over the volume of a sphere or circle (depending upon the system dimension) of diameter

$$\sigma = \left(\sigma_1^d + \sigma_2^d\right)^{1/d}. \tag{19}$$

Many materials are indeed prone to strong deformation after high impact collisions. This is, thus, a reasonable approximation, if the time scale of deformation is small, compared to the mean free time. In any case, given that fractality offers larger collision cross-section, the dynamics of the systems with such spherical structural approximation will be different from those without the approximation. In the rest of the subsection, unless otherwise mentioned, by BAM we will refer to the ballistic aggregation model with circular approximation.

In the BAM, the post-collisional position and velocity of a new cluster can be obtained from the conservation equations related to center of mass and linear momentum. A snapshot during the evolution of a system with such rules is shown in the right frame of Fig. 7(a). Before presenting results on dynamics

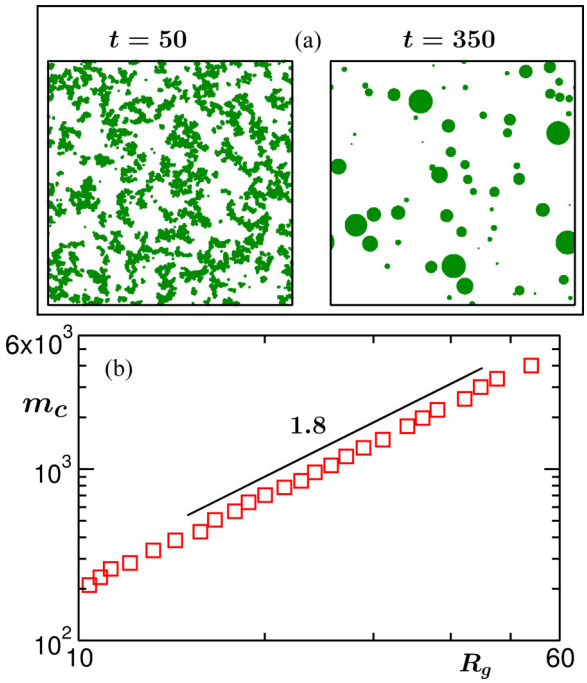

FIG. 7. (a) (Left frame) A snapshot during the evolution of the fractal BAM in $d = 2$ with $L = 512$. See text for details. (Right frame) Same as the left frame but with spherical structural approximation and for $L = 1024$. In both the frames only parts of the original systems are shown. Times are mentioned on top of the frames. (b) Cluster mass, from a typical snapshot, is shown as a function of the radius of gyration, R_g, for the fractal BAM case. The solid line there is a power-law with exponent 1.8. Rest of the results will be presented for $L = 1024$ and spherical BAM.

of this simplified model, in Fig. 7(b) we show data for the fractal dimension corresponding to the snapshot in the left frame of Fig. 7(a). Here we present mass of individual clusters as a function of the radius of gyration (R_g), on a log-log scale. Nice power-law behavior is visible, providing (mass) fractal dimension $d_f \simeq 1.8$. As mentioned above, henceforth we will work with only the circular BAM. Even though the primary aim is to examine a scaling property related to aging, in the following we present accurate results for energy decay and cluster growth as well, from appropriate analyses. To the best of our knowledge, such accurate analyses were not previously performed to draw conclusions on the behavior of these quantities.

In Fig. 8(a) we show a log-log plot of energy as a function of time. A plot for the growth of mass is shown in Fig. 8(b). Power laws can be identified in both the cases. While from these log-log plots it appears that the energy and mass are (approximately) inversely proportional to each other, as predicted in Eq. (2), the inset of Fig. 8(b), where we show kinetic energy as a function of mass, provides a different information. There the exponent of the power-law decay appears clearly higher than unity, approximately 1.15, over a significant range. For an accurate estimate we, thus, calculate the instantaneous exponents [49] for the time dependence of m and E as

$$\theta_i = -\frac{d\ln E}{d\ln t}, \quad \zeta_i = \frac{d\ln m}{d\ln t}. \tag{20}$$

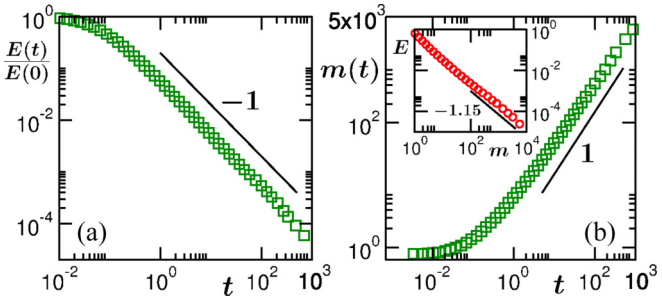

FIG. 8. Log-log plots of the (a) kinetic energy vs. time and (b) mass vs. time, for the $d = 2$ BAM. In the inset of (b) we show a log-log plot of E vs. m. The solid lines in these figures are power-laws, exponents for which are mentioned.

Such exercises were performed for the $d = 1$ BAM as well. However, we avoided presenting those results, since this aspect in $d = 1$ is better understood.

We have plotted θ_i, versus $1/t$, and ζ_i, versus $1/m$, in Figs. 9(a) and 9(b), respectively. In the asymptotic limit we obtain $\theta \simeq 1.08$ and $\zeta \simeq 0.94$. Thus, the predictions of Eq. (2) are not obeyed. These numbers, however, appear consistent with a hyperscaling relation [15] (for ballistic aggregation), which in $d = 2$ has the form

$$\theta + \zeta = 2. \tag{21}$$

The failure of Eq. (2) lies in the fact that at low packing fraction the assumption related to uncorrelated velocity, inherent in the derivation of Eq. (2), breaks down [16]. It is expected that at higher density, where the collision events are more frequent, this prediction will work [15,16,43]. Here we ask the question: is it not possible to obtain the above-mentioned value of ζ from Eq. (16) or (17)? Note that under the spherical approximation $d_f = 2$. Thus, we need to estimate γ to find out the reason for the deviation of ζ from unity [see Eq. (2)].

In the inset of Fig. 9(b), we plot $v_{\rm rms}$ as a function of m. A power-law behavior from the log-log plot can be appreciated. The corresponding exponent ($\gamma \simeq 0.53$) provides $\zeta \simeq 0.97$ [see Eq. (17)]. Even though this number is smaller than 1, no conclusive remark should be made from such small deviation. Following Ref. [16], we state here the reason behind a difference between θ and ζ. Via the introduction of a dissipation parameter (α'), ratio between the kinetic energy

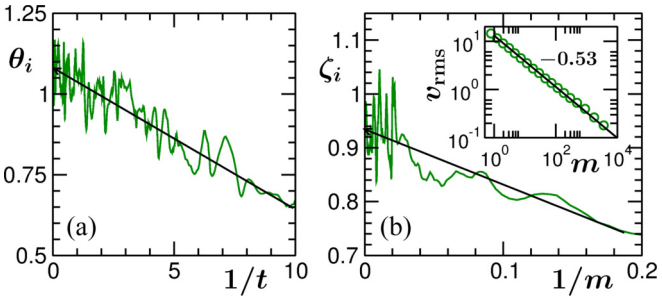

FIG. 9. Plots of (a) θ_i vs. $1/t$ and (b) ζ_i vs. $1/m$, for the 2D BAM. The solid lines are guides to the eye. Inset in (b): Log-log plot of $v_{\rm rms}$ vs. m, for the 2D BAM. The solid line there is a power-law, exponent for which is mentioned next to it.

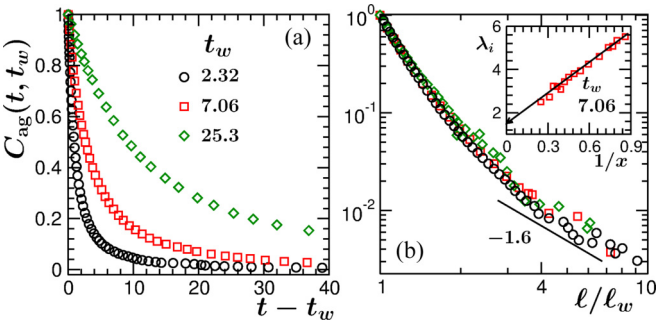

FIG. 10. (a) For the 2D BAM the autocorrelation function $C_{\rm ag}(t,t_w)$ from different values of t_w are plotted vs. $t - t_w$. (b) Log-log plots of $C_{\rm ag}(t,t_w)$ vs. $x(= \ell/\ell_w)$, using data sets of (a). The solid line represents a power-law with exponent $\lambda = 1.6$. In the inset of (b) we show the instantaneous exponent λ_i as a function of $1/x$. The solid line there is related to a linear extrapolation to $x = \infty$.

dissipation in a collision and the mean kinetic energy per particle, these authors showed that $\alpha' = 1$ for high collision frequency. On the other hand, for low frequency, i.e., at low particle density, $\alpha' > 1$. In the latter scenario, the particles with larger kinetic energy, than the mean, undergo more frequent collisions, enhancing the dissipation. This leads to a value of θ higher than unity. This fact becomes more prominent at densities smaller than the one considered here. For example, for $\rho = 0.005$, we find $\theta \simeq 1.15$ and $\zeta \simeq 0.85$. A similar fact is observed in $d = 3$. There, in future, we intend to verify how well the corresponding hyperscaling relation [15] holds. Next, we present results for aging.

In Fig. 10(a) we show plots of $C_{\rm ag}(t,t_w)$, versus $t - t_w$, for a few different values of t_w. Like in $d = 1$, time translational invariance is absent, as expected. It is clearly seen that with increasing age relaxation gets slower. In Fig. 10(b) we show the log-log plots of $C_{\rm ag}(t,t_w)$, as a function of ℓ/ℓ_w. Good collapse of data on a master curve is visible. This confirms the scaling property of Eq. (6). For large values of ℓ/ℓ_w power-law decay becomes prominent. Continuous bending of the master curve for small abscissa variable implies early-time correction to the power-law. The large x data appear consistent with an exponent $\lambda \simeq 1.6$, the number being roughly the same as in the $d = 1$ case. For aging during kinetics of phase transitions, on the other hand, one observes strong dimension dependence of λ [38,39]. Here, note that in $d = 2$ we expect [57] $\beta = 4$. Thus, the (lower) bound in Eq. (9) is 3. This calls for a look at the behavior of the equal-time structure factor for the present problem. This is because, while for bicontinuous domain structures ($d > 1$) the analytical prediction ($\beta = 4$) has been numerically confirmed [57,60], the cases of discrete domain morphology are less studied. Before taking a look at the equal time structure factor, since a violation of the bound appears to be a possibility, in the inset of Fig. 10(b) we plot the instantaneous exponent

$$\lambda_i = -\frac{d\ln C_{\rm ag}}{d\ln x}, \tag{22}$$

as a function of $1/x$, to accurately quantify λ. The data set provides an asymptotic value $\lambda \simeq 1.5$.

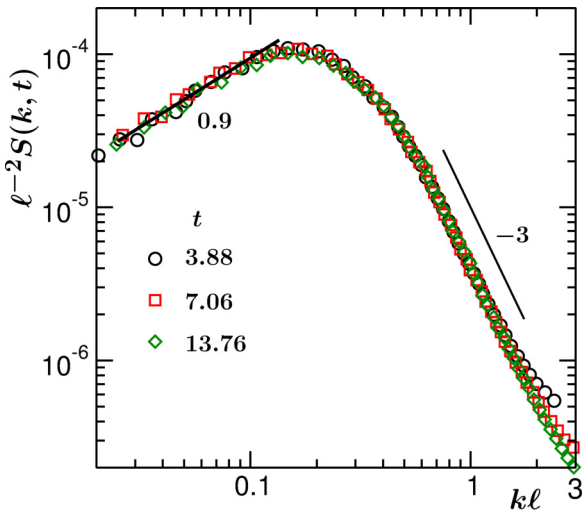

FIG. 11. Log-log plots of $\ell^{-2}S(k,t)$ vs. $k\ell$, for the BAM in $d = 2$. The solid lines are power laws, exponents for which are mentioned on the figure.

In Fig. 11, we present a scaling plot of $S(k,t)$, viz., we show $\ell^{-2}S(k,t)$ versus $k\ell$, on a log-log scale. The large k data are consistent with the power-law exponent -3, which corresponds to the Porod law [54] in $d = 2$ for a scalar order parameter. In the small k region, on the other hand, the enhancement is much weaker than k^4. In fact, in the relevant region, we observe $\beta \lesssim 1$, a number similar to the one we observed in recent studies of kinetics of phase transition with conserved off-critical composition as well, for which one naturally obtains circular or spherical domain structures. In that case, we have the lower bound $\lesssim$1.5, which is satisfied by the above estimated value of λ.

V. CONCLUSION

We have studied kinetics of clustering in GGM and BAM, in $d = 1$ and 2. It is shown that the average size of the clusters grows as power law with time. In $d = 1$, via a dynamic renormalization group theoretical method of analysis [37], the corresponding exponent for the GGM has been identified to be approximately $2/3$, which is in agreement with that for the BAM. In this dimension, for both the models, the growth appears inversely proportional to the energy decay, showing consistency with the scaling predictions of Carnevale *et al.* [21] for ballistic aggregation. The growth mechanism, for the GGM case, has been identified directly by calculating the mean-squared-displacements [53] of the centers of mass of clusters. To avoid the inelastic collapse, for the GGM, in this dimension, we have used a cutoff δ. For relative velocities $<\delta$, the value of e was set to unity for the colliding partners [6]. We observed δ-dependent saturation in the growth of mass, appearing earlier for larger values of δ. Interestingly, in such saturation regime also the energy decay continued to follow the theoretical form $t^{-2/3}$. This calls for further investigation. In $d = 2$, on the other hand, any equivalence between the GGM and the BAM is shown to be absent.

In both the dimensions, for the density field, we have studied the aging property [26,28] for ballistic aggregation, which is first in the literature. It is shown that, like in kinetics of phase transitions, the order-parameter autocorrelation function scales with ℓ/ℓ_w. The asymptotic forms of the scaling functions have been identified to be power laws. The corresponding exponents have been estimated and discussed with reference to the structural property. It is shown that the exponents obey dimension-dependent lower bounds [30], predicted for kinetics of phase transitions. However, unlike in the kinetics of phase transitions, the aging exponents here appear to be very close to the lower bounds, irrespective of the dimension. The similar values of the exponent for the GGM and the BAM cases in $d = 1$, further suggests close equivalence of the dynamics in the two cases, in this dimension. We intend to undertake similar studies in $d = 3$.

With respect to the more realistic ballistic aggregation, the simulations are rather challenging for $d > 1$. This is due to the formation of fractal structures. Because of this reason, like in the existing simulation studies, spherical structural approximation has been used by us. It will be interesting to investigate the scaling properties related to aging and other aspects without such approximation.

ACKNOWLEDGMENTS

The authors thank Department of Science and Technology, Government of India, for financial support. S.K.D. also acknowledges the Marie Curie Actions Plan of European Commission (FP7-PEOPLE-2013-IRSES Grant No. 612707, DIONICOS), International Centre for Theoretical Physics, Trieste, and École Normale Supérieure de Lyon for partial support. S.P. is thankful to UGC, India, for support through a research fellowship.

[1] I. S. Aranson and L. S. Tsimring, Rev. Mod. Phys. **78**, 641 (2006).
[2] N. V. Brilliantov and T. Poeschel, *Kinetic Theory of Granular Gases* (Oxford University Press, Oxford, 2004).
[3] I. Goldhirsch and G. Zanetti, Phys. Rev. Lett. **70**, 1619 (1993).
[4] R. Brito and M. H. Ernst, Europhys. Lett. **43**, 497 (1998).
[5] S. Luding and H. J. Herrmann, Chaos **9**, 673 (1999).
[6] E. Ben-Naim, S. Y. Chen, G. D. Doolen, and S. Redner, Phys. Rev. Lett. **83**, 4069 (1999).
[7] X. Nie, E. Ben-Naim, and S. Chen, Phys. Rev. Lett. **89**, 204301 (2002).
[8] S. K. Das and S. Puri, Europhys. Lett. **61**, 749 (2003).
[9] S. K. Das and S. Puri, Phys. Rev. E **68**, 011302 (2003).
[10] M. Shinde, D. Das, and R. Rajesh, Phys. Rev. Lett. **99**, 234505 (2007).
[11] M. Shinde, D. Das, and R. Rajesh, Phys. Rev. E **84**, 031310 (2011).
[12] A. Bodrova, A. K. Dubey, S. Puri, and N. V. Brilliantov, Phys. Rev. Lett. **109**, 178001 (2012).
[13] S. Paul and S. K. Das, Europhys. Lett. **108**, 66001 (2014).
[14] E. Trizac and J.-P. Hansen, Phys. Rev. Lett. **74**, 4114 (1995).
[15] E. Trizac and J.-P. Hansen, J. Stat. Phys. **82**, 1345 (1996).

[16] E. Trizac and P. L. Krapivsky, Phys. Rev. Lett. **91**, 218302 (2003).
[17] A. Lipowski, D. Lipowska, and A. L. Ferreira, Phys. Rev. E **73**, 032102 (2006).
[18] P. K. Haff, J. Fluid Mech. **134**, 401 (1983).
[19] O. Herbst, R. Cafiero, A. Zippelius, H. J. Herrmann, and S. Luding, Phys. of Fluids **17**, 107102 (2005).
[20] W. C. Germs, K. Guo, R. A. J. Janssen, and M. Kemerink, Phys. Rev. Lett. **109**, 016601 (2012).
[21] G. F. Carnevale, Y. Pomeau, and W. R. Young, Phys. Rev. Lett. **64**, 2913 (1990).
[22] N. Brilliantov, P. L. Krapivsky, A. Bodrova, F. Spahn, H. Hayakawa, and V. Stadnichuk, Proc. Natl. Acad. Sci. U.S.A. **112**, 9536 (2015).
[23] M. Hummel and M. G. Mazza, Phys. Rev. E **93**, 022905 (2016).
[24] A. J. Bray, Adv. Phys. **51**, 481 (2002).
[25] A. Onuki, *Phase Transition Dynamics* (Cambridge University Press, Cambridge, UK, 2002).
[26] M. Zannetti, in *Kinetics of Phase Transitions*, edited by S. Puri and V. Wadhawan (CRC Press, Boca raton, FL, 2009).
[27] J. Midya and S. K. Das, Phys. Rev. Lett. **118**, 165701 (2017).
[28] D. S. Fisher and D. A. Huse, Phys. Rev. B **38**, 373 (1988).
[29] F. Liu and G. F. Mazenko, Phys. Rev. B **44**, 9185 (1991).
[30] C. Yeung, M. Rao, and R. C. Desai, Phys. Rev. E **53**, 3073 (1996).
[31] M. Henkel, A. Picone, and M. Pleimling, Europhys. Lett. **68**, 191 (2004).
[32] F. Corberi, E. Lippiello, A. Mukherjee, S. Puri, and M. Zannetti, Phys. Rev. E **85**, 021141 (2012).
[33] S. Ahmad, F. Corberi, S. K. Das, E. Lippiello, S. Puri, and M. Zannetti, Phys. Rev. E **86**, 061129 (2012).
[34] S. Majumder and S. K. Das, Phys. Rev. Lett. **111**, 055503 (2013).
[35] M. Hummel, J. P. D. Clewett, and M. G. Mazza, Europhys. Lett. **114**, 10002 (2016).
[36] A. Baldassarri, U. M. B. Marconi, and A. Puglisi, Phys. Rev. E **65**, 051301 (2002).
[37] C. Roland and M. Grant, Phys. Rev. B **41**, 4663 (1990).
[38] J. Midya, S. Majumder, and S. K. Das, J. Phys.: Condens. Matter **26**, 452202 (2014).
[39] J. Midya, S. Majumder, and S. K. Das, Phys. Rev. E **92**, 022124 (2015).
[40] S. Majumder, J. Zierenberg, and W. Janke, Soft Matter **13**, 1276 (2017).
[41] M. P. Allen and D. J. Tildesley, *Computer Simulation of Liquids* (Clarendon, Oxford, 1987).
[42] D. C. Rapaport, *The Art of Molecular Dynamics Simulations* (Cambridge University Press, Cambridge, UK, 2004).
[43] S. N. Pathak, Z. Jabeen, D. Das, and R. Rajesh, Phys. Rev. Lett. **112**, 038001 (2014).
[44] S. McNamara and W. R. Young, Phys. Rev. E **50**, R28 (1994).
[45] C. S. Campbell, Annu. Rev. Fluid Mech. **22**, 57 (1990).
[46] S. Luding and S. McNamara, Gran. Matter **1**, 113 (1998).
[47] C. V. Raman, Phys. Rev. **12**, 442 (1918).
[48] S. Majumder and S. K. Das, Phys. Rev. E **81**, 050102 (2010).
[49] D. A. Huse, Phys. Rev. B **34**, 7845 (1986).
[50] N. Goldenfeld, *Lectures on Phase Transitions and the Renormalization Group* (Addison-Wesley, London, 1992).
[51] S. K. Das and S. Puri, Phys. Rev. E **65**, 026141 (2002).
[52] S. N. Pathak, D. Das, and R. Rajesh, Europhys. Lett. **107**, 44001 (2014).
[53] J.-P. Hansen and I. R. McDonald, *Theory of Simple Liquids* (Academic Press, London, 2008).
[54] G. Porod, *Small-Angle X-Ray Scattering*, edited by O. Glatter and O. Kratky (Academic Press, New York, 1982).
[55] Y. Oono and S. Puri, Mod. Phys. Lett. B **2**, 861 (1988).
[56] S. N. Majumdar, D. A. Huse, and B. D. Lubachevsky, Phys. Rev. Lett. **73**, 182 (1994).
[57] C. Yeung, Phys. Rev. Lett. **61**, 1135 (1988).
[58] H. Furukawa, Phys. Rev. B **40**, 2341 (1989).
[59] P. Ramanlal and L. M. Sander, Phys. Rev. Lett. **54**, 1828 (1985).
[60] S. Ahmad, S. K. Das, and S. Puri, Phys. Rev. E **85**, 031140 (2012).